Effect of Dopant Concentration and Solution pH on the Structural and Optical Properties of Electrodeposited Manganese-Doped Zinc Selenide Thin Films

Alhassan D. Yusuf [a*] and Donald N. Okoli [b]

[a] *Department of Physics Education, Federal College of Education (Technical), Umunze, Nigeria.*
[b] *Department of Physics and Industrial Physics, Nnamdi Azikiwe University, Awka, Nigeria.*

Authors' contributions

This work was carried out in collaboration between both authors. Both authors read and approved the final manuscript.

Article Information

Original Research Article

ABSTRACT

The study has been carried out to investigate the influence of manganese concentration and solution pH on the structural and optical properties of electrodeposited Mn-doped ZnSe thin films. The study adopted an experimental research type using lab apparatus to grow and ZnSe/Mn thin films. Manganese doped ZnSe thin films have been deposited on well cleaned fluorine-doped tin oxide (FTO) coated conducting glass substrates at room temperature via two-electrode potentiostatically electrodeposition technique. All deposition was carried out at room temperature of $25^{o}C$. Prepared solutions of $Mn(NO_2)_3.5H_2O$, $ZnSO_4.7H_2O$ and hydrogen selenide as sources of Mn^{2+}, Zn^{2+} and Se^{2-} ions respectively were used. The Mn concentrations have been varied by varying the molar concentration of $Mn(NO_2)_3.5H_2O$ in the solution as 0.0, 0.1, 0.2 and 0.3 mol %. Ammonia (NH_3) solution has been used to adjust the pH of the solution (as pH 7.0, 7.5, 8.0 and 8.5). The samples thickness has been obtained electromechanically by a profilometer measurement. X-ray diffraction studies revealed eight (8) diffraction peaks oriented along (110), (101), (200), (211), (220), (310), (301) and (321) planes, indicating that all the deposited films were polycrystalline in nature with mixture of cubic zinc blende and hexagonal structures with the most preferred orientation along (211) plane. The average crystallite size calculated increases as the Mn concentration and solution temperature increases. Optical studies revealed a direct band gap

Corresponding author: Email: alhassanyusuf08@gmail.com;

transition with the energy value decreases (as 3.56, 3.43, 3.39 and 2.92 eV) as the Mn contents increases, and increases (as 3.39, 3.91, 3.96 and 3.88 eV) with increase in the solution pH. The optical conductivity of the grown thin films was in the range of 2.87 – 3.32 x10^{14} s^{-1}. The synthesized thin films could find potential application in photo sensing, optoelectronic and hetero-junction solar cells devices.

Keywords: Thin film; electrodeposition; ZnSe; manganese; band gap.

1. INTRODUCTION

The inclusion of d-elements doped IIB-VIA semiconductor thin films in all categories of electronic structures has drawn a considerable interest, owing to the believes that with specific impurities atoms introduce into the binary compound could alter the microcrystalline structures and thus yields new material systems with physiochemical properties different from the host material. The group 3d-transition metals (such as Cr, Fe, Co, Cu, Mn e.t.c) – doped II-VI semiconductors, have in particular drawn a great attention as it offers a great opportunity to integrate optical, electrical and magnetic properties into a single material, making them ideal candidates for magneto–optical, non–volatile memory,- spintronic and optoelectronic devices [1,2,3]. In addition, these metals have no solubility limit in the host material [4].

Among the group II-VI binary compounds as host materials, ZnSe has drawn major attention due to its unique physical properties, such as wide and direct energy bandgap in the range 2.6–3.1eV, high refractive index, transparency over a wide range of visible spectrum, ability of emitting light in the blue-green region [5, 6, 7], and relatively large value of nonlinear optical coefficients [8]. Zinc Selenide can be crystallized principally in both cubic and hexagonal structures. It has electrical resistivity of the order 10^4-10^{12}Ωcm [7]. ZnSe and its lattice matched ternary alloys have been regarded as important member of II–VI compound semiconductors for various applications [9]. It has shown a wide range of applications in the field of optoelectronic devices such as blue-green light emitting diode, blue laser diode, laser screens, thin film transistors, photo detectors, photo diodes, dielectric mirrors, non-linear optical, photovoltaic cells and as window material for thin film hetero-junction solar cells [10,11,9].

Different dopants have been used to dope ZnSe thin films, these include iron [12,13,14], indium [8,15,16], tellurium [17], aluminum [18], Bismuth [19], nitrogen [20], Chromium [21], silver [22,23], europium [24], Tin [9], cobalt [3,26], copper [25,26], manganese [27,28].

Various techniques have been employed to prepare thin films of doped ZnSe, including thermal evaporation [8,29], lasers assisted evaporation [18,21,22], closed space sublimation [23,25], chemical bath [15,28,30], electro-chemical [12,13,20,24], but based on current needs to fabricate semiconductor devices on variable substrate sizes and shapes, to ensure low energy consumption, and to reduce material wastage and system damage, electrodeposition (ED) method has been adopted for this present studies for the fabrication of ZnSe/Mn thin films. From the available literature reports, there no particular empirical studies on the electro-deposited ZnSe/Mn thin films. The present study is therefore focused on investigating influences of Mn concentration and solution pH on the Structural and optical properties of ZnSe/Mn thin films for their potential applications in various optoelectronic devices.

2. MATERIALS AND METHODS

2.1 Materials

The materials used for the growth and characterization of ZnSe and ZnSe/Mn thin films included; power supply, carbon electrode, fluorine doped tin oxide (FTO) substrates, potentiostat which supplies a DC voltage in a two-electrode cell setup, digital weighing balance, digital hand held pH meter (HL7300) with pH value of 7.0, G & G electronic scale, magnetic stirrer, stop watch, Digital multimeter, thermometer 0-750°C, 756S UV-VIS spectro-photometer, Bruker D8 Advance X-ray diffractometer with Cu Kα line (λ= 1.54056Å).

The chemical used included; Zinc tetraoxo-sulphate (VI) heptahydrate (ZnSO$_4$.7H$_2$O), manganese nitrate pentahydrate (Mn(NO$_2$)$_3$.5H$_2$O), Selenium powder (Se), Hydrogen Chloride (HCl), Ammonia solution (NH$_3$), Deionized water. All chemicals used were of Analytical Grade.

2.2 Experimental Details

Thin films of manganese-doped zinc selenide (ZnSe/Mn) have been deposited onto flourine-doped tin oxide (FTO) coated conducting glass substrates. Before the deposition, attention has been paid on the cleaning and activating the substrate surfaces, the substrates have been dipped in acetone, methanol, rinsed with distilled water and later ultrasonicated for 30 mins in acetone solution after which they were rinsed in distilled water again and kept in an oven to dry. All the prepared substrates have been kept in air-tight container.

A 0.1M aqueous solutions of $ZnSO_4.7H_2O$ and $Mn(NO_2)_3.5H_2O$ as sources of Zn and Mn ions have been prepared by dissolving 5.7508 g of each in 100 ml of deionized water. 5 ml of HCl has been first used to dissolve the selenium metal powder to form hydrogen selenide (H_2Se). 0.1M concentration aqueous solution of the H_2Se has been then prepared by dissolving 8.0969 of it in 100 ml of deionized water.

The deposition has been carried out when 20ml of the prepared solutions of $ZnSO_4.7H_2O$ and H_2Se, and 10ml of $Mn(NO_2)_3.5H_2O$ have been poured into the electrochemical bath system with constant stirring. The Mn concentrations have been varied by varying the molar concentration of Mn $(NO_2)_3.5H_2O$ in the solution as 0.0, 0.1, 0.2 and 0.3 mol %. Ammonia (NH_3) solution has been used to adjust the pH of the solution (as pH 7.0, 7.5, 8.0 and 8.5) using digital hand held pH meter (HL7300). The deposition has been allowed to take place potentiostatically using a two-electrode configuration under – 200 mV deposition potential, at constant voltage of 10V and room temperature of 25^oC for 10s after which the coated slides were withdrawn from the bath, rinsed with distilled water and dried in air. The samples have been characterized for structural and optical properties.

2.3 Theoretical Methodology

2.3.1 Structural

The inter-planar distance, d_{hkl} has been calculated by using the Brag equation as,

$$d_{hkl} = \frac{\lambda}{2sin\theta} \tag{1}$$

The Cubical lattice constant, a has been calculated using the equation:

$$a = d_{hkl} \, x \, \sqrt{h^2 + k^2 + l^2} \tag{2}$$

From the cubic lattice parameter obtained have been used to compute lattice parameter, *c* for hexagonal structure by the equation,

$$c = \frac{l}{\sqrt{\frac{1}{a^2} - \frac{4}{3}\left(\frac{h^2+k^2+l^2}{a^2}\right)}} \tag{3}$$

The crystallite size, *D* of the deposited films has been computed can b using Scherrer formula [23],

$$D = \frac{k\lambda}{\beta cos\theta} \tag{4}$$

Where, *k* is a shape factor (scherrer constant) with the value 0.94 [7], β is the full width half maximum (FWHM) value of the observed diffraction peaks.

The microcrystalline stain, ε has been calculated using the equation [31],

$$\varepsilon = \frac{\beta_{2\theta}cos\theta}{4} \tag{5}$$

Where, $\beta_{2\theta}$ is the full width half maximum (FWHM) value of the observed diffraction peaks. The dislocation density, ρ in the thin samples has been calculated by using the equation [32],

$$\rho = \frac{15\varepsilon}{aD} \tag{6}$$

The number of crystallites per unit area, *N* within the crystalline structure has been calculated by the equation [33],

$$N = \frac{t}{D^3} \tag{7}$$

Where, t is the thickness of the film sample. The internal stress, S developed within the films has been calculated using the equation [34],

$$S = \frac{\gamma}{1-E} \cdot \varepsilon \qquad (8)$$

Where, γ is the Young Modulus and E is the Poisson ratio of the ZnSe samples, whose values are 67.2 Gpa and 0.28 respectively [31].

2.3.2 Optical

The photon energy, E measured in electron volt (eV) varies with its wavelength, λ (nm) by the relation.

$$E = \frac{1240}{\lambda} \qquad (9)$$

The transmittance, T is calculated from the observed absorbance data by the relation [35],

$$T = \frac{1}{10^A} \qquad (10)$$

Where, A is the absorbance. The absorption coefficient, α is calculated using Beer Lanbert's formula given by [35],

$$\alpha = 2.303 \frac{A}{t} \qquad (11)$$

Where, t is the film thickness.

The bandgap energy is obtained using the relation given by [36],

$$\alpha h v = B(h v - E_g)^{\frac{1}{2}} \qquad (12)$$

By plotting graph of $(\alpha h v)^2$ versus photon energy ($h v$) and extrapolating the straight line portions of the plot to the absolute value of zero, the intercept of the straight line with the $h v$ axis defines the value of the band gap energy [37].

The extinction coefficient, k is computed using the equation [35],

$$k = \frac{\alpha \lambda}{4\pi} \qquad (13)$$

The reflectance and extinction coefficient data have been used to compute the refractive index, n using the equation [35],

$$n = \sqrt{\frac{4R}{(1-R)^2} + k^2} \qquad (14)$$

The optical conductivity, σ_o is calculated using equation [38],

$$\sigma_o = \frac{\alpha n c}{4\pi} \qquad (15)$$

Where, c is the speed of light in vacuum.

3. RESULTS AND DISCUSSION

The results of the structural and optical characterizations of the prepared ZnSe/Mn thin films are discussed in details under the influences of dopants concentration and solution pH.

3.1 Structural Properties

Crystalline structure of the electrodeposited thin film samples have been studied by using a Bruker AXS X-ray diffractometer D8-Advance mounted with 1.5406 wavelength Cu-K$_\alpha$ monochromator. From the peak search-and-match process, the obtained XRD profile data best matched the databases with references (JCP2-41-1445 and JCP2-46-1088), where the Millar indices of the diffraction peaks have been obtained. The XRD patterns of all the prepared thin films are presented in (Figs. 1 and 2) under concentration (0.0, 0.1, 0.2 & 0.3 mol %) and pH (of 7.0, 7.5, 8.0 & 8.5) variations. For all the prepared thin films, the XRD pattern showed eight diffraction peaks oriented along (110), (101), (200), (211) (220), (310), (301) and (321) planes, corresponding to the average value of 2θ as 26.55^o, 33.76^o, 37.76^o, 51.52^o, 54.58^o, 61.60^o, 65.56^o, 78.33^o respectively, indicating that all the deposited films are polycrystalline in nature with mixture of cubic zinc blende and hexagonal structures [3, 9, 22, 28] with preferred orientation along (211) plane. The peak along (101) plane is due to hexagonal wurtzite structure of the stable ZnSe phase as regard to variation in dopant concentration [8, 24] as evident in (Fig.1).

However, Fig. 2 indicates that the ZnSe hexagonal phase is not stable to change in solution pH, as evident in the change in the peak intensity and position, which could be attributed to the variation in reaction kinetics with pH.

The data extracted from the XRD plots are subjected to computation for details analysis of the structural properties of the prepared thin films, and are presented in (Tables 1 and 2). Generally, the hexagonal portions in the crystalline structure of the prepared ZnSe/Mn

thin films are in the ranges, $a = 3.747 – 3.766$ Å and $c = 4.589 – 4.612$ Å. Similar hexagonal lattice parameter ($a = 3.805$ Å and $c = 6.123$ Å) is also reported for ZnSe thin films prepared by electrodeposition method [36]. A tetragonal lattice structure of ZnInSe thin films with lattice parameter of $a = 5.698$ Å and $c = 11.510$ Å had also been reported previously [8].
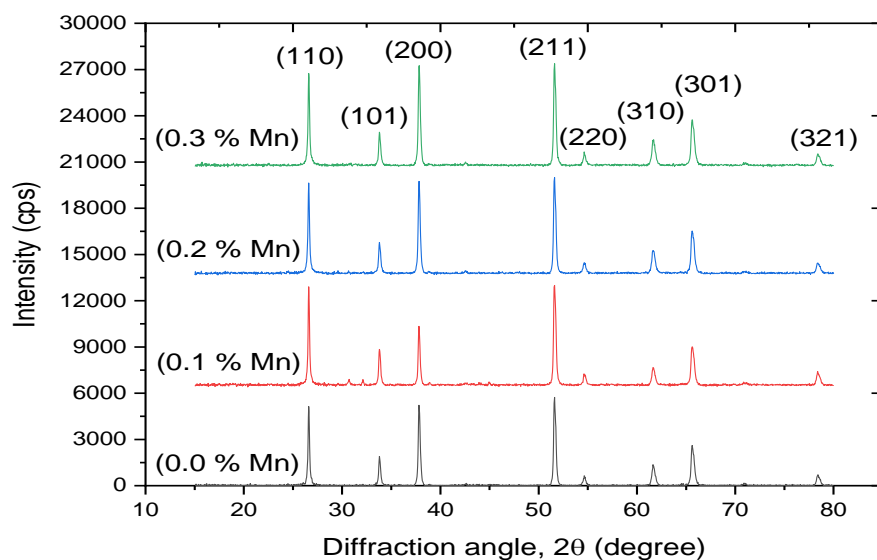

Fig. 1. XRD pattern of the grown ZnSe/Mn thin films under dopant concentration variation
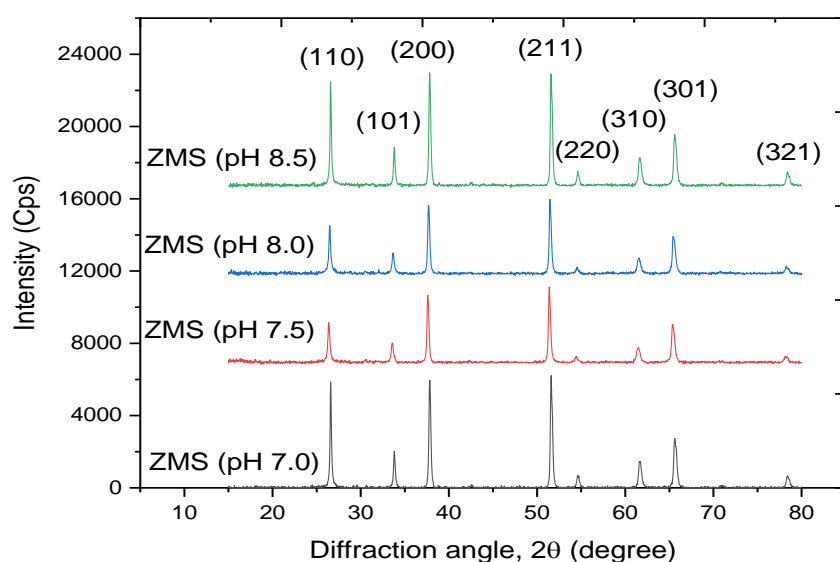

Fig. 2. XRD pattern of the grown ZnSe/Mn thin films under solution pH variation

Table 1. Variation of the XRD average measurement data of the prepared ZnSe/Mn thin films with Mn concentration

Sample Mn conc. (mol %)	*d* (Å)	*a* (Å)	*c* (Å)	D (nm)	N x10^{-17} (cm^{-2})	E x10^{-4}	P x10^{-18} (cm^{-2})	S x107 (pa)
Cubic Structure								
0.0	1.903	4.627	-	39.26	2.12	9.21	7.63	8.60
0.1	1.903	4.628	-	39.61	2.00	9.12	7.48	8.51
0.2	1.906	4.634	-	41.20	1.77	8.81	6.98	8.23
0.3	1.908	4.638	-	42.01	1.60	8.64	6.91	8.07
Hexagonal Structure								
0.0	2.65	3.747	4.589	41.57	1.78	8.71	9.39	8.13
0.1	2.65	3.747	4.589	41.57	1.74	8.71	9.39	8.13
0.2	2.65	3.747	4.589	41.57	1.69	8.71	9.39	8.13
0.3	2.65	3.747	4.589	41.57	1.65	8.71	9.39	8.13

Table 1 indicated that in the case of the cubic structures of the grown ZnSe/Mn thin films, the average lattice constant and crystallite size increase continuously, while the average number of crystallites, strain, dislocation density and the stress developed in the films decrease as the concentration of manganese ions in the solution increases. Similar observations are reported previously on the thin films studies of ZnSe doped with In [8], Ag [23], Eu [24]. In contrast, Al-doped ZnSe thin films studies by the ref.[22], revealed decrease in both lattice constant and grain size, and increase in strain and defect density as the Al content increases. In the case of the wurtzite lattice structure present in the samples, the Table 1 indicated that the crystalline parameters remain unchanged as the Mn concentration increases, confirming the stable binary phase of ZnSe [8], as it is also evident in (Fig. 1).

In Table 2, the average lattice constant and crystallite size of the ZnSe/Mn thin films first decrease as the solution pH value increases (from 7.0 to 7.5), and then increase subsequently, as the pH value increases up to 8.5. The increase in the crystallite size with pH value is also reported [39]. The average number of crystallites per area, strain, dislocation density and the stress developed in the thin films first increase as the solution pH increases (from 7.0 to 7.5), and then decrease subsequently as the pH value increases up to 8.5. These observations indicated that solution pH influences the crystallinity ZnSe/Mn thin films. In the case of the hexagonal portion, crystalline parameters indicated a slight variation as the solution pH increases (see also Fig. 2), which could be attributed to the change in reaction kinetic leading to variation in the stoichiometry of the films [40].

Table 2. Variation of the XRD average measurement data of the prepared ZnSe/Mn thin films with solution pH

Sample Sample pH	*d* (Å)	*a* (Å)	*c* (Å)	D (nm)	N x10^{-17} (cm^{-2})	E x10^{-4}	P x10^{-18} (cm^{-2})	S x107 (pa)
Cubic Structure								
7.0	1.906	4.634	-	41.20	1.77	8.81	6.98	8.23
7.5	1.903	4.628	-	39.18	1.99	9.25	7.68	8.64
8.0	1.904	4.629	-	39.40	1.91	9.20	7.57	8.58
8.5	1.905	4.632	-	40.18	1.78	9.03	7.30	8.43
Hexagonal Structure								
7.0	2.650	3.747	4.589	41.57	1.69	8.71	9.39	8.13
7.5	2.663	3.766	4.612	41.55	1.66	8.71	9.35	8.13
8.0	2.660	3.762	4.607	41.55	1.62	8.71	9.36	8.13
8.5	2.652	3.751	4.594	41.57	1.59	8.71	9.38	8.13

3.2 Optical Properties

The optical properties of all the electrodeposited thin films samples have been studied by using 756S UV-VIS spectrophotometer in the Scanning wavelength range of 300 to 1100 nm at room temperature. From the absorbance data generated the optical parameters are determined. Fig. 3 and 4 represent the absorption spectra of ZnSe/Mn thin films, where the bandgap energy values are extracted and presented in Table 3.

The Table 3 shown that the band gap decreases continuously as the concentration of Mn ions increases. Similar decreases in energy bandgap of ZnSe thin films doped with Cu [21], Ag [23], and Eu [24] have been reported previously. However, increase in bandgap with Mn concentration in ZnS thin films had also been reported previously [37,41].

The decrease in the energy bandgap of the samples with Mn concentration may be linked to the overlapping of energy levels [23] brought about by the increase in the Mn impurity atoms in the films. In addition, as the Mn doping level increases more Mn enter the ZnSe lattice as donor or acceptor atoms and interact with each other forming wider donor band within the bandgap that pushes the Fermi energy level into the conduction or valence band, thereby decreasing the forbidden energy bandgap of the ZnSe/Mn samples. The decrease of the bandgap in spite of the decreased in the films thickness could also be attributed to the formation of big crystallites size [42].
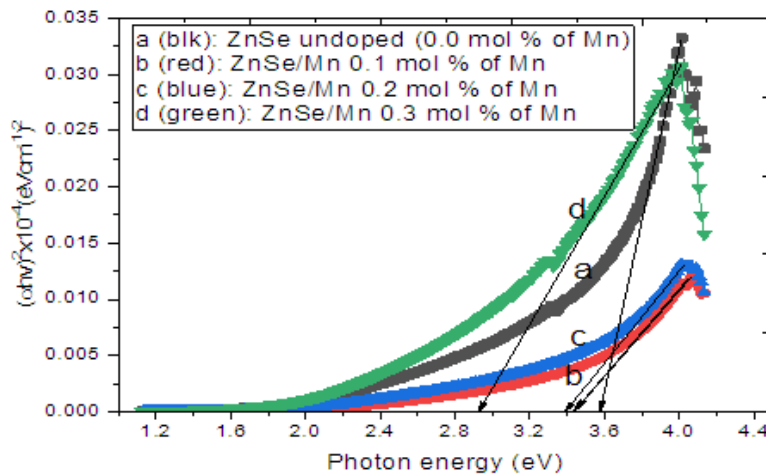

Fig. 3. the ($\alpha h v$)^2 versus photon energy of the grown ZnSe/Mn thin films under concentration variation
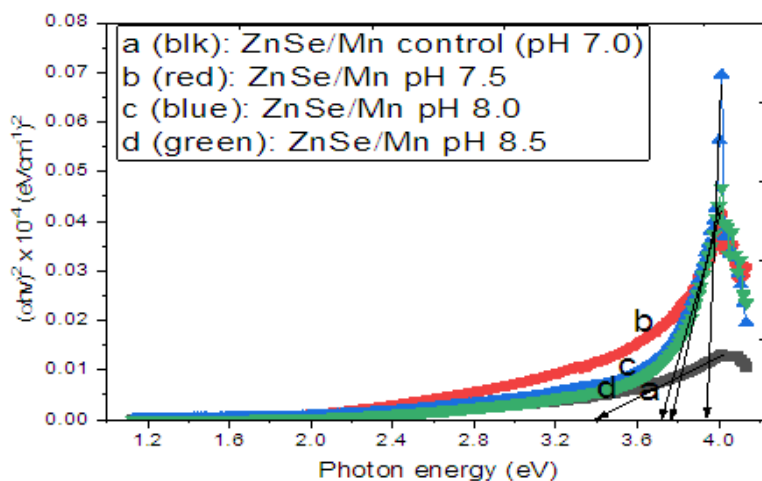

Fig. 4. the ($\alpha h v$)^2 versus photon energy of the grown ZnSe/Mn thin films under solution pH variation

Table 3. Variation of optical bandgap energy of all the prepared ZnSe/Mn thin films with concentration and solution pH

Sample	Thickness (nm)	E_g (eV)
Dopant Concentration		
0.0	128.03	3.56
0.1	124.80	3.43
0.2	121.52	3.39
0.3	118.24	2.92
Solution pH		
7.0	121.52	3.39
7.5	118.92	3.91
8.0	116.41	3.96
8.5	113.96	3.88

In the case of solution pH, Table 3 also revealed that the band gap increases continuously as the solution pH increases up to 8.0, and then drops eventually as the pH increases further to 8.5. in the studies of Co-doped ZnSe thin films also revealed a decrease of band gap with increase in pH values [3].This pattern of observation of band gap relationship with pH has been also reported (as 3.67, 3.81, 3.88 and 3.78 eV corresponded to the pH values of 11.50, 10.99, 10.31 and 10.00 respectively) by Ben-Nasr [43] on the study of ZnS thin films. However, decrease in band gap with pH values had been reported on ZnSe thin films [39]. The increase in the bandgap with increase in pH values may be explained based on the fact that when the film thickness reduces, it may rendered the crystal with scanty number of atoms and conduction electrons, which in turn reduces the number of impurity states or band width within the bandgap, hence increasing in band gaps of the ZnSe/Mn thin films with pH value.

The Figs. 5 and 6 represent the transmittance spectra of the prepared ZnSe/Mn thin films. It is generally observed that the transmittance increases smoothly with photon wavelength from a very low value in UV to a maximum value in infra-red spectrum region [31].

In Fig. 5, it is revealed that the transmittance first increases and then drops subsequently as the Mn ions concentration increases over the visible spectrum. Decrease in transmittance with Mn concentration is also reported previously [37, 41]. The decrease in transmittance with Mn ions concentration could be attributed to the increase in absorbance due to the excessive density doping resulted from increasing Mn contents in the films which consequently decreases transmittance.

In Fig. 6, it is revealed also that the transmittance first drops and then increases subsequently as the pH value increases over the visible spectrum. The continue increase in transmittance with increase in pH is reported also on ZnS thin film [43]. This observation in the visible region could also be related to the change in the crystalline structure of the ZnSe/Mn thin films (see also Table 2).

The Figs. 7 and 8 represent the refractive index versus wavelength for all the prepared thin films. Within the visible region, the refractive index increases sharply with photon wavelength and then remains nearly saturated at the infra-red region. Another general important observation is the interference effects on the spectra of the refractive indices for all the deposited films, indicating optical properties dependent on the photon wavelength. Similar interference behaviour on various optical spectra had been reported previously [8, 16, 31]. In addition, the spectra also reveal a direct relation between the refractive index and optical transmittance at the visible region [1].

In Fig. 7, it is revealed that the refractive index of the ZnSe/Mn samples first increases (blue shifted in peak) and then decreases subsequently (with red shifted in peak) as the Mn concentration increases over the visible spectrum. However, the infra-red region indicated a reverse trend as the Mn concentration increases. The drop in the refractive index with Mn concentration in the visible region may be attributed to the decrease in the ZnSe/Mn films thickness. While the observation in the IR region could be attributed to change in transmittance (see also Fig. 7).

In Fig. 8, it is also revealed that the refractive index of the ZnSe/Mn samples first drops (with red shifted) and then increases subsequently (with blue shifted in peak) as the pH increases over the visible spectrum. However, the infra-red

region indicated the reverse trend as pH increases. The observation in the visible region could be linked to the variation of the crystalline structure of the ZnSe/Mn thin films, which can be explained based on the fact that as larger crystallites break to form multiple numbers of smaller grains, bonds are broken and some atoms that have acquired energy beyond the average got lost out of the crystals lattice, consequently making the crystalline films a little less dense. Hence, the reason for the initial drops in the refractive index. When the crystallites become bigger in size, the refractive index of the films gets increased.
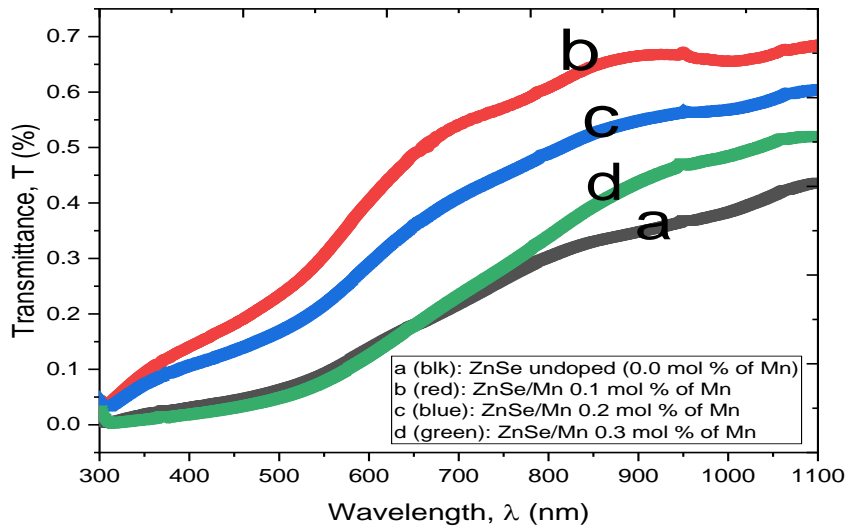
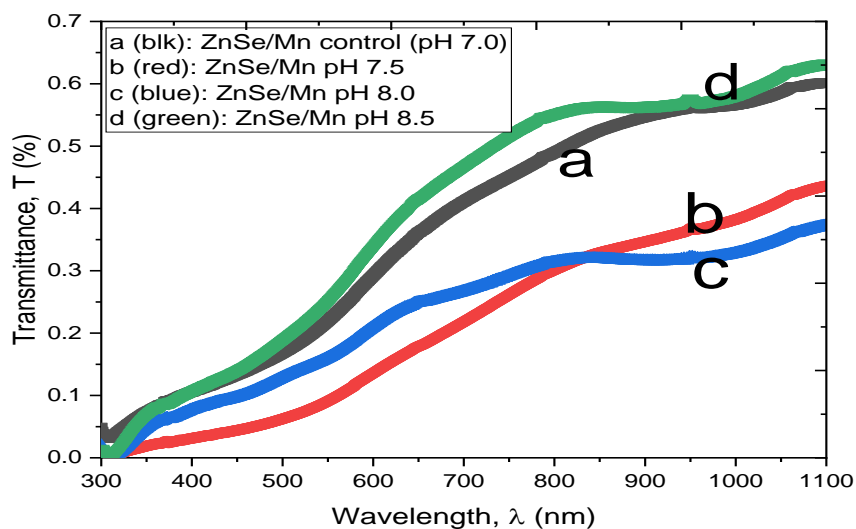**Fig. 5. Transmittance spectrum of the grown ZnSe/Mn thin films under solution pH variation**

Fig. 6. Transmittance spectrum of the grown ZnSe/Mn thin films under solution pH variation
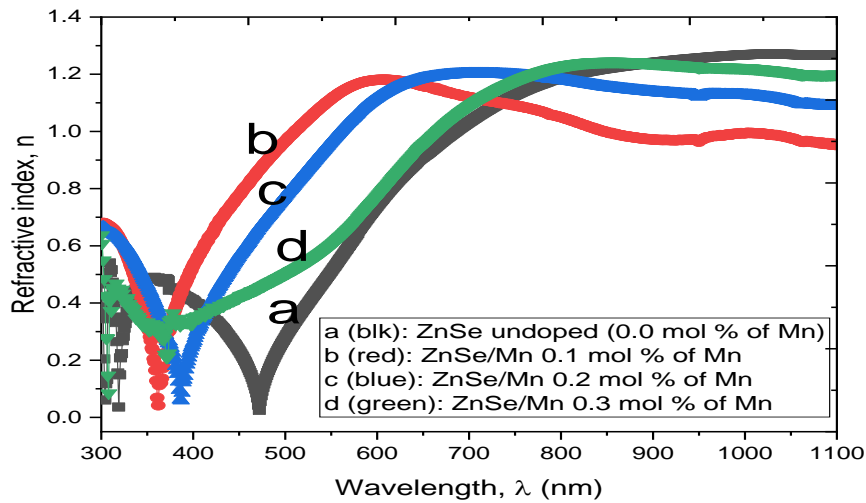
Fig. 7. Refractive index versus wavelength of the grown ZnSe/Mn thin films under concentration variation
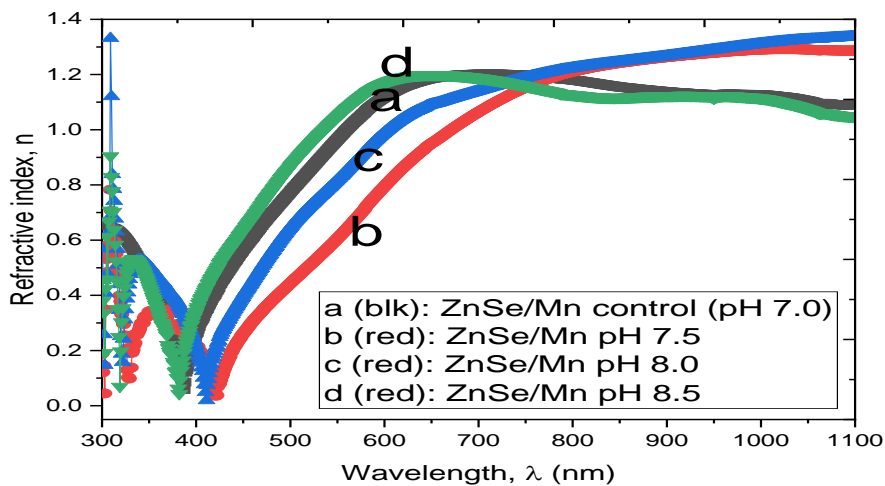

Fig. 8. Optical conductivity versus wavelength of the grown ZnSe/Mn thin films under concentration variation

The Figs. 9 and 10 represent the optical conductivity also known as AC conductivity versus wavelength for all the prepared ZnSe/ Mn thin films. In overall the optical conductivities of all the prepared thin films are high in UV-Vis region and low in IR region. Similar observation is reported on ZnS:Mn thin films [45]. The nature of observations here reveals that the prepared thin films absorbs the entire UV region and transmit the Vis-IR region.

In Fig. 9, it is revealed that the optical conductivity of the ZnSe/Mn samples first drops from 3.03 to 2.69 $\times 10^{14} s^{-1}$ (with blue shifted in peak), and then increases subsequently to 3.32 $\times 10^{14} s^{-1}$ (with red shifted in peak) as the Mn ions content increases over the Vis region. The increase in optical or AC conductivity with Dopant concentration could be attributed to the loss in dielectric nature of the prepared ZnSe/Mn thin films as a result of increase in carrier conduction and dipole motion of charged atoms.
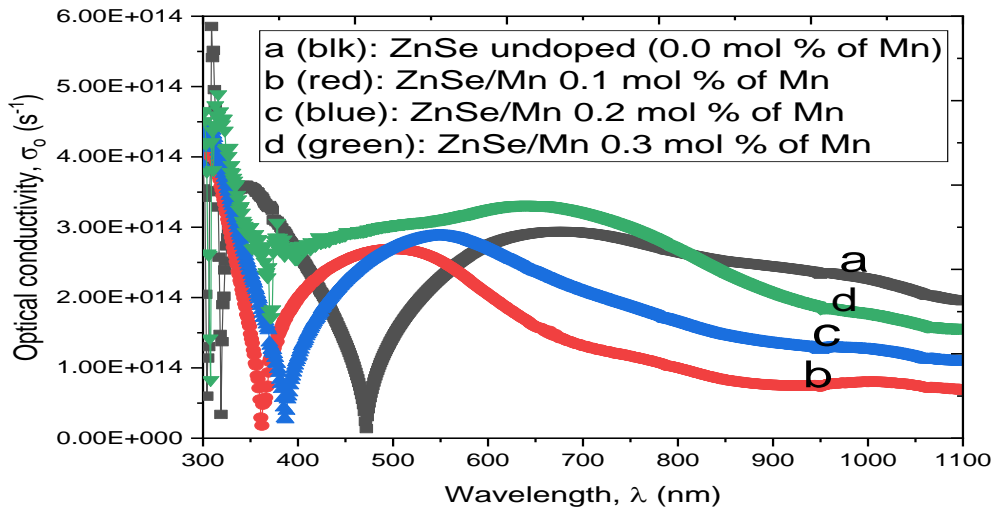
Fig. 9. Optical conductivity versus wavelength of the grown ZnSe/Mn thin films under concentration variation
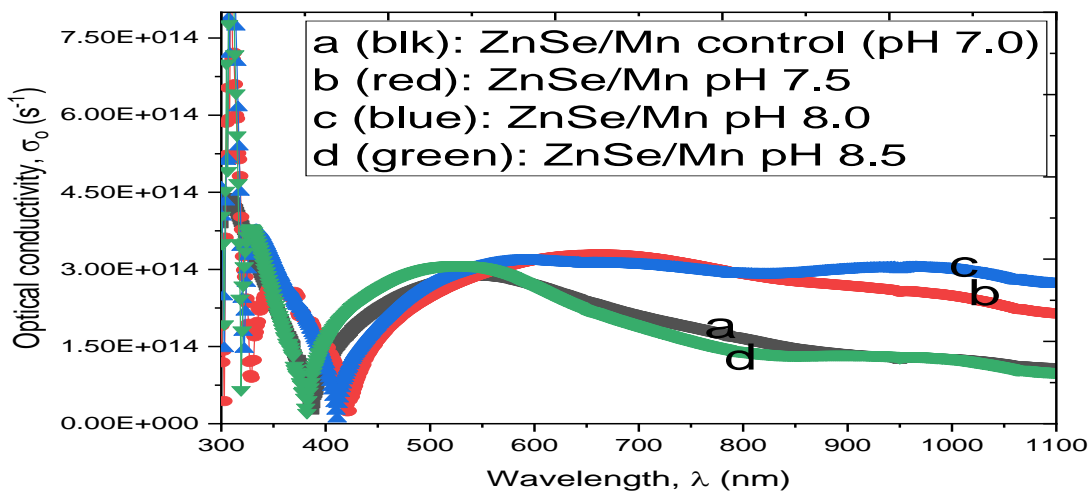

Fig. 10. Optical conductivity versus wavelength of the grown ZnSe/Mn thin films under solution pH variation

In Fig. 10, it is also revealed that the optical conductivity of the ZnSe/Mn samples increases slight from 2.87 to 3.29 $\times 10^{14} s^{-1}$ (with red shifted in peak), and then drops subsequently to 3.09 $\times 10^{14} s^{-1}$ (with blue shifted in peak) as the pH increased over the Vis region. Decrease in optical conductivity with pH had also been reported on Co-doped ZnSe thin films [3]. In contrast, the studies of Tin doped ZnSe thin films revealed increase in optical conductivity as pH increases [9]. The decrease in the A.C

conductivity with increase in pH could be link to the decrease in the thickness of the prepared ZnSe/Mn thin films.

4. CONCLUSION

The results presented in this work prove that there is a possibility to perform doping of zinc selenide thin films with Mn impurities using electrodeposition method. According to the results obtained from the present studies, the

optimal deposition conditions for the preparation of the ZnSe/Mn thin films include; temperature, pH value and Mn precursor (dopant) concentration of 25°C, 7.0 and 0.3M respectively. At these conditions, the bandgap energy value (2.92 eV) and lattice constant of 4.6379 Å which are closest to that of the bulk ZnSe crystals have been obtained. In addition, well crystalline films with bigger grain sizes (in the range, 41. 20 – 42.01 nm) are obtained under these conditions. The films properties may also be improved further when subjected to annealing.

It has been observed also that the thickness of all the prepared thin films decreases continuously as the values of the deposition parameters (concentration and pH) increases. This feature could have significant influences on the various properties of the grown samples. The XRD studies show the presence of well crystallized nanocrystalline particles having mixture of cubic and hexagonal structures. The optical transition in the films has been found to be direct. The resulting wide band gap coupled with wide range of optical transparency make it suitable for short wavelength optoelectronic device applications such as, for blue laser diodes, laser screens, thin film transistors, photo detectors, photovoltaic cells and hetero structures for solar cells. The high optical conductivity value of 10^{14} s^{-1} of the prepared ZnSe/Mn thin films implied that they have good photo response and could be applied as photon conductor.

DISCLAIMER

The products used for this research are commonly and predominantly use products in our area of research and country. There is absolutely no conflict of interest between the authors and producers of the products because we do not intend to use these products as an avenue for any litigation but for the advancement of knowledge. Also, the research was not funded by the producing company rather it was funded by personal efforts of the authors.

COMPETING INTERESTS

Authors have declared that no competing interests exist.

REFERENCES

1. Okafor PC, Ekpunobi AJ. Effect of manganese percentage doping on optical propertiesof zinc sulphide (ZnS) nanofilms prepared by electrodeposition method. International Journal of Scientific & Engineering Research. 2016;7(2):169-173.

2. Hassanzadeh, J., Shayeshe, FS. & Ziabari, A A. Effects of pH on the optical properties of doped CdS (Cu, Fe) nanoparticles in TG as a Capping Agent. ACTA Physica Polonica A. 2014;120: 713-716.

3. Ikhioya, IL, Onal, EO, Maaza M, Ezema, F. Influence of precursion pH on the optical and electrical properties of electrochemical deposited cobalt doped ZnSe thin films for photovoltaic application. Current Research in Green and Sustainable Chemistry. 2022;5:100286.

4. Masaaki, T. Recent progress in ferromagnetic semiconductors and spintronics devices. Japanese Journal of Applied Physics. 2021;60:010101. https://doi.org/10.35848/13474065/abcadc

5. Okereke WA, Ezenwa IA, Ekpunobi AJ. Effect of thickness on the optical propertiesof zinc selenide thin films. Journal of Non-Oxide Glasses. 2011;3(3):105-111.

6. Oztas M, Bedir M, Bakkaloglu OF, Ormanci, R. Effect of Zn:Se ratio on the properties of sprayed ZnSe thin films. ACTA PHYSICA, A. 2005;107(3):525- 534.

7. Pathan HM, Lokhande, CO. Deposition of metal chalcogenide thin films by successive ionic layer adsorption and reaction (SILAR) method. Bulletin Material Science. 2004; 27(2): 85 – 115.

8. Gullu HH. Material and device characterization of ZnInSe$_2$ and Cu$_{0.5}$Ag$_{0.5}$InSe$_2$ thin films for photovoltaic applications. Dissertation for degree of doctor of philosophy in physics submitted to the Graduate School of Natural and Applied Science of East Techinical University; 2016. (In press).

9. Ikhioya IL, Okoli DN, Ekpunobi AJ. Influence of precursion pH on the optical and electrical properties of electrochemical deposited cobalt doped ZnSe thin films for photovoltaic application. International Journal of ChemTech Research. 2019;12(5):200- 211

10. Antohe S, Ion L, Girtan T. Optical and morphological studies of thermally vacuum evaporated ZnSe thin films. Roman Reports in Physics. 2013;65(3):805-811.

11. Namikawa Y. ZnSe single crystals grown by vapor growth methods and their applications. SEI Technical Review. 2011;72.

12. Lohar GM, Thombare JV, Shinde SK, Chougale UM, Fulari VJ. Preparation and characterization of iron doped zinc selenide thin film by electrodeposition. Journal of Shivaji University (Science and Technology). 2015;41(2):1-3.

13. Lohar GM, Shinde SK, Rath MC, Fulari VJ. Structural, optical, photoluminescence, electrochemical, and photoelectrochemical properties of Fe doped ZnSe hexagonal nanorods. Material Science Semiconductors Process. 2014;26:548–554.

14. Moraes AR, Mosca DH, Schrenier WA, Mattoso N, Silveira E. Structural and chemical properties of ZnSe-Fe electrodeposited granular films. Brazilian. Brazilian Journal of Physics. 2002;32(2):383.

15. Babu P, Reddy MV, Revathi N, Reddy KTR. Effect of pH on the physical properties of ZnIn2Se4 thin films grown by chemical bath deposition. Journal of Nano- and Electronic Physics. 2011;3: 38-91.

16. Gordillo G, Calderon C, Rojas F. Determination of optical constants of $ZnIn_{1-x}Se$ thin films deposited by evaporation. Rev. Mex. Fis. 20003;49(1): 329-334.

17. Tkachenko IV. Mechanisms of defect formations and luminescence in undoped and tellurium doped crystals of zinc selenide. Dissertation for Ph.D. degree in physics and mathematics. Chernivtsi; 2005. (In press).

18. Choudhury MGM, Islam MR, Rahman MM, Hakim MO, Khan MKR, Kao KJ et al. Preparation and characterization of ZnSe:Al thin films. Acta Physica Slovace. 2004;54(4):417.

19. Shen Y, Xu N, Hu W, Sun J, Ying Z, Wu J. Bismuth doped films fabricated on silicon substrates by pulsed laser deposition. Solid-State Electronics. 2008;52(11):1833-1836.

20. Manzoli A, Eguiluz KIB, Salazar-Banda GR, Machado SAS. Electrodeposition and characterization of undoped and nitrogen-doped ZnSe films. Material Chemistry and Physics. 2010;121:58–62.

21. Williams JE. Growth of Chromium-Doped zinc selenide Thin films by pulsed laser deposition for mid-infrared applications. A PhD dissertation in the University of Alabama; 2010. (In press).

22. Kayed TS, Qasraw AF, Elsayed KA. Structural, optical, dielectric and electrical properties of Al-Doped ZnSe thin films. Journal of Electronic Materials. 2019;48(6). htts://doi-org/10.1007/511664-019-07055-3.

23. Nazar AS, Mussart A, Wagar AS, Waqar M. Physical properties of silver doped ZnSe thin films for photovoltaic applications. Iranica Journal of Energy & Environment. 2014;5(1):87-93.

24. Manikandan D, Jeyachandran V, Manikandan A. Effect of Eu^{3+} ions on structural, opticaland morphological properties of electrochemically deposited ZnSe thin films. International Journal of Pure and Applied Mathematics. 2018;119(12):3799-3821.

25. Arslan M, Muhammad R, Mahmood A, Rasheed R. Effect of thermal annealing on the physical properties of $Zn_{1-x}Cu_xSe$ thin films deposited by close spaced sublimation technique. ACTA Metallurgical Sinica (English Letters). 2013;26(6):699-706.

26. Ali Z, Agili AK, Maqsood A, Akhtar SJ. Properties of Cu-doped Low Resistive ZnSefilms deposited by two-Sourced Evaporation. Vacuu. 2005;80(4):302-309.

27. Makhniy VP, Kinzerskaya OV, Horlay PP, Ul'yanitskiy KS. Optical properties of diffused ZnSe:Mn layers. Yuri Fedkovycl Chernivtsi National University, 2 Kosyubynskyst. Chernivtsi, Ukraine. 2007;58012. (In press).

28. Kumar TR, Vedamalai M. Growth of Mn^{2+} ions doped ZnSe thin films by Chemical bath deposition and their characterization. International Journal of Pure and Applied Mathematics. 2018;119(12):6839-6849.

29. Bushra HH, Iman HK, Mohammed HM, Auday HS. Effect of V, In, and Cu doping on properties of p-type ZnSe/Si heterojunction solar cell. Progressing Industrial Ecology. An International Journal. 2019;13(2):173-186.

30. Sirkeli VP, Nedeoglo DD, Nedeoglo ND, Radevici IV, Sobolevskaia RL, Sushkevich KD, et al. Magnetic and luminescent properties of manganese-doped ZnSe crystals. Physica B; 2012. www.elsevier.com/locate/physb.

31. Andalipa I, Chitra D, Shamima C, Mehaz S, Tahmina B. Structural and optical characterization of vacuum evaporated zinc selenide thin films. European Scientific Journal. 2014;10(15):1857-1881.

32. Desai HN, Dhimmar JM, Modi BP. Study of linear and non-linear optical parameters of

Zinc selenide thin films. International Journal of Engineering Research and Application. 2016;5(6): 117-122.

33. Ojo AA, Dharmadasa IM. Electroplating of semiconductor materials for applications in large area electronics: A Review Coatings. 2018;8:262.
DOI:10.3390/coatings8080262.

34. Nix, WD. Mechanical properties of thin films. Lecture Notes. Materials Science and Engineering 353, Stanford University, Stanford. 2005. (in press).

35. Buba ADA. Optoelectronic Properties of Zinc Selenide (ZnSe). Thin films deposited using chemical bath deposition (CBD) technique. British Journal of Applied Science & Technology. 2016;14(3):1-7.

36. Ayeshamariam A, Kashif M, Muthuraja S, Jegadeswari S, Saravanakkumar D, Alhaji NMI, et al. Optical characterization of ZnSe thin films by using electrodeposition technique. International Journal of Emerging Technology and Advanced Engineering. 2014;4(5):584-590.

37. Muslimin ES, Stepanus S, Amiruddin KB. Optimization of optical propertiesof ZnS:Mn thin films deposited by co-evaporation electron beam. Asian Journal of Scientific Research. 2019;12:60-64

38. Bhavsar V, Tripathi D. Study of refractive index dispersion and optical conductivity of Polypyrrole doped PVC films. Indian Journal of Pure & Applied Physics. 2016; 54:105-110.

39. Shikha D, Mehta V, Sharma JK, Sharma J. The influence of pH on properties of nanocrystalline ZnSe thin films. Optoelectronics and Advanced materials 5 –Rapid Communications. 2016;10(3-4):196–200.

40. Pandurang CP, Santosh TM, Rangrao VS, Lalasaheb PD. Structural, morphological and optical studies of ZnSe thin films growth using chemical bath. Pelagia Research Library, USA: Advances in Applied Science Research. 2013;4(3):177-181.

41. Ozutok F, Erturk K, Bilgin V. Growth electrical and optical study of ZnS:Mn thin films. ACTA Physical Polonica A. 2012;121(1):221-223.

42. Khairnar U, Behere SP. Optical properties of polycrystalline Zinc Selenide thin films. Materials Sciences and Applications. 2012;3:36-40.

43. Ben-Nasr T, Kamoun N, Kanzari M, Bennaceur R. Effect of pH on the properties of ZnS thin films grown by chemical bath deposition. Thin Solid Films. 2006;500:4–8.

44. Miah MAH, Begum J, Momin B. Influence of thickness on the structural and optical properties of ZnSe thin films. Journal of Applied Science and Technology. 2010;7(2):27-32.

45. Okafor PC, Ekpunobi AJ, Ekwo PA. Effect of manganese percentage doping on thickness and photoconductivity of zinc sulphidenano films prepared by electrodeposition method. International Journal of Science and Research. 2013; 4(12):2275-2279.